Markov Chain Model of Emitter Activations in Superresolution Microscopy

Yi Sun

Electrical Engineering Department
The City College of City University of New York
New York, NY 10031, USA
ysun@ccny.cuny.edu

Abstract— In superresolution microscopy (SRM), it is desired to establish a well-reasoned model of data movie so that an advanced localization algorithm can be developed to achieve a high quality of SRM images. A model of data movie can be composed of a model of data frame and a model of emitter activation process. We previously developed a model of data frame. In this paper, we focus on modeling of emitter activation process. Both continuous and cycled illuminations are considered. While Markov chains are considered for the former, no model is developed for the latter. First, a three-state Markov chain is adopted for the continuous illumination. The state transition probabilities are derived from the first order of kinetics for the emitter activation process. The stationary probabilities of states are derived when an emitter is photoactivatable. Second, a novel state transition diagram for the cycled illumination is proposed. The state transition probabilities are derived for both the activation frames and deactivation frames. Incorporating the model of emitter activation process and the model of data frames, the models of data movie for both the continuous and cycled illuminations in 2D and 3D imaging are simulated by custom MATLAB codes. The results show that the models can well synthesize a data movie of SRM, thus providing a means to be broadly utilized in simulating SRM systems, evaluating quality of SRM images, and testing performance of localization algorithms.

Keywords—Single molecule localization microscopy, single molecule imaging, data model, emitter activation, Markov chain

I. INTRODUCTION

Superresolution microscopy (SRM), e.g., PALM [1], STORM [2], FPALM [3], and dSTORM [4], employs photoactivatable molecules as emitters to trade off the temporal resolution with a super spatial resolution, thus enabling to view the ultrastructure of a biological sample at a nanoscale. A camera takes a data movie that consists of a number of frames on which the point spread function (PSF) images of the activated emitters in each frame are presented. A localization algorithm is employed to estimate the emitter locations from the data movie and yields an SRM image of the estimated emitter locations. The localization algorithm plays an important role in obtaining a high quality of SRM images [5] [6].

It is desired to establish a well-reasoned model of the data movie, and then an advanced localization algorithm can make use of the model to achieve a high accuracy in emitter localization. A model of an SRM data movie is usually composed of two parts [7]. First, the data frame is modeled to

This research was partly supported by Army Research Office under Grant Number W911NF-23-1-0189 and NSF under Grant Number 2313072.

incorporate all parameters of the SRM system except the emitter activation process. Second, the process of emitter activations is modeled. The combination of them constitutes a model of a data movie. The first part is well modeled in [8] [9]. This paper will focus on the model and analysis of the second part. Simulations to generate data movies with 2D and 3D imaging will be carried out to include both parts.

II. MODEL OF EMITTER ACTIVATIONS

There are two types of illuminations to activate emitters, i.e., the continuous illumination and the cycled illumination. In a continuous illumination, as adopted in PALM [1], FPALM [3], and dSTORM [4], a single photoswitchable molecule serves as an emitter. In a cycled illumination, as adopted in STORM [2], a pair of conjugated photoswitchable molecules are employed to serves as an activator and an emitter, respectively.

The process of emitter activations is usually modeled by a Markov chain with the two on and off states in [10], the three on, off, and photobleached states in [11], and the four on, meta-off, off, and photobleached states in [12], and generally *J* states in [7]. The state transition probabilities are unspecific. Moreover, these models consider only the continuous illumination. In this paper, modeled are both the continuous and cycled illuminations.

A. Continuous Illumination

In the continuous illumination, the emitters are illuminated continuously by an excitation laser. The mth emitter is randomly independently switched to the on state denoted by $a_m(t) = 1$ for a random time T_1 during which the emitter emits photons. Then it is switched to the off state denoted by $a_m(t) = 0$ for a random time T_0 during which it does not emit photons. The emitter is alternately switched to the on and off states as shown in Fig. 1 until photobleached. The photobleached state is denoted by $a_m(t) = 2$.

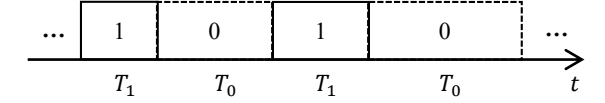


Fig. 1. The activation state $a_m(t)$ for the mth emitter.

The activation of a fluorescence molecule satisfies the first order of kinetics [13] [14], that is, both T_0 and T_1 are exponentially distributed and depend on the excitation laser power. Let the means of T_0 and T_1 be t_0 and t_1 , respectively. The probability density function of T_i for i = 0, 1 is

$$p_i(t) = (1/t_i)\exp(-t/t_i).$$
 (1)

Consider a frame time Δ_t during which the mth emitter is in the photoactivatable state. In the condition that the mth emitter is in the state i for i=0,1 at the beginning of a frame, the probability that it remains the same state through the end of the frame is $p_i = \Pr(T_i \ge t_i)$, that is

$$p_i = \exp(-\Delta_t/t_i). \tag{2}$$

Let T_2 be the random time during which the mth emitter is photoactivatable. That is, during the time $t \le T_2$, the emitter can emit photons when activated. Assume that T_2 is exponentially distributed with a mean t_2 and the probability density function is

$$p_2(t) = (1/t_2)\exp(-t/t_2).$$
 (3)

The pair of states 0 and 1 can be considered as a composite photoactivatable state. In the condition that the *m*th emitter is in the photoactivatable state at the beginning of a frame, the probability that the emitter remains in the photoactivatable state through the end of the frame is

$$p_2 = \exp(-\Delta_t/t_2). \tag{4}$$

The transition probability from the photoactivatable state, either state 0 or state 1, to the photobleached state is equal to $1 - p_2$.

Clearly, if the *m*th emitter is in the state i at the beginning of a frame, the probability that it remains the same state through the end of the frame is equal to $p_i p_2$ for i = 0, 1. Conversely, the transition probability from state i to 1 - i for i = 0, 1 is equal to $(1 - p_i)p_2$.

With the exponential distribution, the random variables T_0 , T_1 , and T_2 are memoryless, that is, the state transition from each of states 0, 1, and 2 depends only on the current state and is independent of the previous states, which is a property of a Markov chain. Denote by $a_m(n)$ the state of the mth emitter in the nth frame. Then $a_m(n)$ is a Markov chain as shown in Fig. 2 where the self-transition of state 2 is omitted.

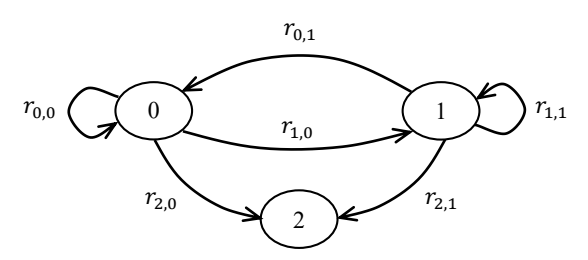


Fig. 2. State transition diagram of the Markov chain $a_m(n)$.

Let $r_{j,i} = \Pr[a_m(n+1) = j | a_m(n) = i]$ be the transition probability from state i to state j for i, j = 0, 1, 2. Then the state transition probabilities can be expressed in terms of the probability density functions of T_0 , T_1 , and T_2 as

$$\begin{cases}
r_{0,0} = p_0 p_2, & r_{1,0} = (1 - p_0) p_2, r_{2,0} = 1 - p_2, \\
r_{0,1} = (1 - p_1) p_2, r_{1,1} = p_1 p_2, & r_{2,1} = 1 - p_2,
\end{cases} (5)$$

 $r_{0,2} = r_{1,2} = 0$, and $r_{2,2} = 1$. The state transition probabilities are determined by parameters t_i for i = 0, 1, 2 through three

probabilities p_0 , p_1 , and p_2 . The state transition matrix can be easily written according to Eq. (5).

The four transition probabilities $r_{j,i}$ for i, j = 0, 1 in Eq. (5) describe the state transition in the composite photoactivatable state, that is, the emitter is not photobleached yet. The two probabilities $r_{2,i}$ for i = 0, 1 describe the transition from a photoactivatable state to the photobleached state.

State 2 is an absorbing state and therefore the Markov chain is transient and does not have stationary probabilities for states 0 and 1. States 0 and 1 construct a two-state Markov chain that alone is obviously irreducible, recurrent, and aperiodic, and therefore has a stationary probability for each state of 0 and 1, i.e., $\beta_i = \Pr[a_m(n) = i]$ for i = 0, 1. By applying the principle that the back and furth flows from one state to another must be equal in the stationary Markov chain, it is easy to obtain that

$$\beta_0 = \frac{1 - p_1}{2 - p_0 - p_1}, \qquad \beta_1 = \frac{1 - p_0}{2 - p_0 - p_1}. \tag{6}$$

With approximation, the result is applicable to the case that the transition probability from the composite photoactivatable state to the photobleached state is sufficiently small, i.e., $1 - p_2 \approx 0$.

For a data movie of N frames, let P_n be the probability that an emitter is photobleached in the nth frame. For $1 \le n \le N$,

$$P_n = p_2^{n-1}(1 - p_2) (7)$$

is the probability of n-1 photoactivatable frames followed by the photobleached frame. For n > N,

$$P_{N+1} = p_2^N (8)$$

is the probability that the emitter is photobleached after the *N*th frame or the emitter is photoactivatable in the entire movie. The average number of photoactivatable frames per emitter equals

$$N_2 = \sum_{n=1}^{N} (n-1)P_n + NP_{N+1} = \frac{p_2(2 - p_2 - p_2^N)}{1 - p_2}.$$
 (9)

Then the average number of activations or the average number of frames that an emitter is activated in the data movie is approximately equal to

$$M_{ae} \cong \beta_1 N_2. \tag{10}$$

The average total number of activations for all *M* emitters in the data movie is approximately equal to

$$M_{at} \cong \beta_1 M N_2. \tag{11}$$

The probability that an emitter is photoactivatable in the nth frame is equal to the probability that the emitter is photoactivatable in all frames from 1 to n, that is, p_2^n . The activation processes of all M emitters are mutually independent. The average number of activated emitters in the nth frame for $1 \le n \le N$ approximately equals

$$M_a(n) \cong \beta_1 p_2^n M. \tag{12}$$

B. Cycled illumination

In a cycled illumination [2], a pair of conjugated fluorescence molecules is attached to ultrastructure of a

biological sample, one of which serves as an activator and the other serves an emitter. In the beginning of each cycle, for a short time which is usually one frame time, a low-power laser (e.g., a green laser in [2]) excites the activator that by the Forster resonance energy transfer (FRET) [14] switches the emitter to the on state with a probability. In the activation frame, usually no data frame is taken. In several following deactivation frames, another high-power laser (e.g., a red laser [2]) switches the emitter to the off state with a probability, and the data frames are taken by a camera. The illumination is operated cycle by cycle as shown in Fig. 3.

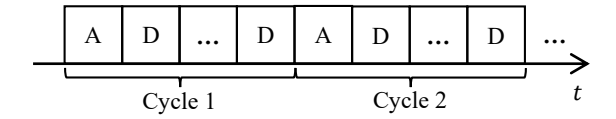


Fig. 3. A cycled illumination. Each cycle consists of one A-frame followed by *K* D-frames.

In an activation frame A, denote by T_{Ai} for i = 0, 1 the times of off and on states, respectively, which are exponentially distributed with the means t_{Ai} . The probability that the state retains unchanged during an A-frame is equal to

$$p_{Ai} = \exp(-\Delta_t/t_{Ai}). \tag{13}$$

Correspondingly, the probability of a state transition is equal to $1 - p_{Ai}$.

Similarly, in a deactivation frame D, denote by T_{Di} for i = 0, 1 the times of off and on states, respectively, which are exponentially distributed with the means t_{Di} . The probability that the state retains unchanged during the D-frame is equal to

$$p_{Di} = \exp(-\Delta_t/t_{Di}). \tag{14}$$

The probability of a state transition is equal to $1 - p_{Di}$.

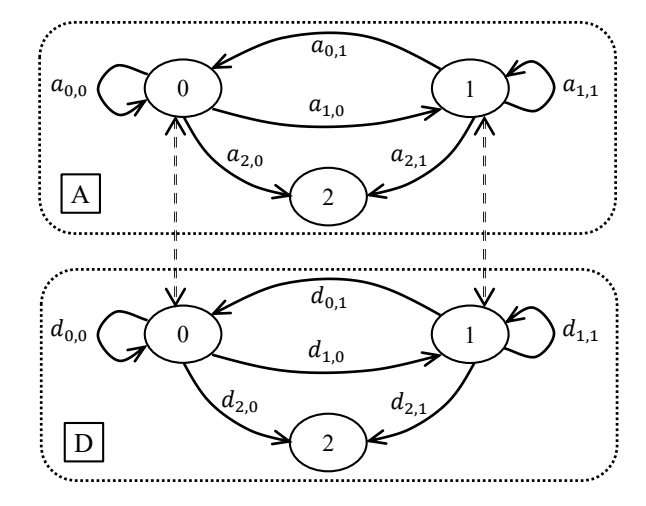


Fig. 4. The state transition diagram corresponding to the cycled illumination in Fig. 3. The states 0's, 1's, and 2's are identical in the A-frame and in the D-frame. In an A-frame, the state transits according to the upper diagram denoted by the squared A. In a D-frame, the state transits according to the lower diagram denoted by the squared D. At the end of the A-frame, the states are moved from the A-diagram to the D-diagram At the end of the Kth D-frame, the states are moved from the D-diagram to the A-diagram.

In general, the laser powers are properly set up so that an emitter has the following activation behavior. In an A-frame, a 0-state is more likely to transit to a 1-state, i.e., $1-p_{A0}>p_{A0}$ or $p_{A0}<0.5$. That is, $t_{A0}<\Delta_t/\ln(2)\cong 1.4427\Delta_t$. On the other hand, in a D-frame, a 1-state is more likely to transit to a 0-state, i.e., $1-p_{D1}>p_{D1}$ or $p_{D1}<0.5$, i.e., $t_{D1}<\Delta_t/\ln(2)\cong 1.4427\Delta_t$.

The photoactivatable time T_2 is exponentially distributed with the mean t_2 . Same as in the continuous illumination, the probability for an emitter to be photoactivatable in both states 0 and 1 in an A-frame as well as in a D-frame is identical and equal to p_2 .

Fig. 4 shows the state transition diagram of the cycled illumination where the self-transitions of state 2 are omitted. The state transition probability from a i-state to itself is $a_{i,i}$ in an Aframe and $d_{i,i}$ in a D-frame for i = 0, 1. Thus, the state transition can be expressed by a two-phase diagram with the state transition probability as

$$\begin{cases} a_{0,0} = p_{A0}p_2, & a_{1,0} = (1 - p_{A0})p_2, a_{2,0} = 1 - p_2, \\ a_{0,1} = (1 - p_{A1})p_2, a_{1,1} = p_{A1}p_2, & a_{2,1} = 1 - p_2, \end{cases}$$
(15)

 $a_{0,2} = a_{1,2} = 0$, and $a_{2,2} = 1$ for A-frames and

$$\begin{cases} d_{0,0} = p_{D0}p_2, & d_{1,0} = (1 - p_{D0})p_2, d_{2,0} = 1 - p_2, \\ d_{0,1} = (1 - p_{D1})p_2, d_{1,1} = p_{D1}p_2, & d_{2,1} = 1 - p_2, \end{cases}$$
(16)

 $d_{0,2}=d_{1,2}=0$, and $a_{2,2}=1$ for D-frames. The state transition probabilities are determined by the five parameters t_{A0} , t_{A1} , t_{D0} , t_{D1} , t_2 through p_{A0} , p_{A1} , p_{D0} , p_{D1} , and p_2 .

III. SIMULATIONS

Two simulations are carried out to generate data movies based on the model. One is for the continuous illumination with 2D imaging, and the other is for the cycled illumination with 3D imaging. The frame model in [8] [9] are considered. Simulations are carried out by custom codes in MATLAB.

A. Continuous Illumination

In the simulation of continuous illumination with 2D imaging, the 2D Gaussian PSF is applied. The following parameter values are employed. (a) Data frame: The wavelength for Alexa 700 is $\lambda = 723$ nm, and numerical aperture is $N_a =$ 1.40. The standard deviation of the 2D Gaussian PSF is estimated from the Airy PSF and is equal to $\sigma = 1.3238/\alpha \cong$ 108.81 with $\alpha = 2\pi N_a/\lambda$ [15]. The size of the field of view is $L_x = L_y = 4096$ nm, pixel size is $D_x = D_y = 128$ nm, and frame size is $K_x = K_y = 32$ pixels. Frame time is $D_t = 0.01$ sec, emitter intensity is I = 300000 photons/sec, and the average photon count per frame per emitter is $D_t I = 3000$ photons. The mean of Poisson noise is b = 5, and then $\gamma_p =$ 60000 and the signal to Poisson noise ratio (SPNR) is SPNR = $10\log_{10}(0.07912\,\gamma_p/\sigma^2) \cong -3.97$ (dB) [15]. The Gaussian noise has mean $\mu = 5$ and variance G = 3 photons/sec/nm², and then $\gamma_q = 100000$ and the signal to Gaussian noise ratio (SGNR) is SGNR = $10\log_{10}(0.07912 \gamma_a/\sigma^2) \approx -1.75$ (dB) [15]. Furthermore, the ratio of emitter intensity and total noise is $\gamma = 37500$ and then the total signal to noise ratio (SNR) is SNR = $10\log_{10}(0.07912 \gamma/\sigma^2) \cong -6.01$ (dB) [15], which is

in the range of middle SNRs in practice. (b) *Emitters*: M = 500emitters are located on a 2D helix. The distance between adjacent emitters is 40 nm. (c) Emitter activation process: The data movie has N = 500 frames, and then the acquisition time is $D_t N = 5$ sec. The mean time of emitter deactivation is $t_0 = 0.3$ sec, and then $p_0 = 0.967$. The mean time of emitter activation is $t_1 =$ 0.2 sec, and then $p_1=0.607$. The mean time of photoactivatable emitter is $t_2=5$ sec, and then $p_2=0.998$. Then the state transition probabilities are $r_{0,0} = 0.965$, $r_{1,0} =$ 0.033, $r_{0,1} = 0.393$, $r_{1,1} = 0.605$, $r_{2,0} = 0.002$, and $r_{2,1} = 0.002$ 0.002. The state 0 has a probability $\beta_0 = 0.923$, and the state 1 has a probability $\beta_1 = 0.077$. Then the average number of photoactivatable frames per emitter by Eq. (9) is $N_2 = 316.742$, and its value in simulation is 314.260. The average number of activations per emitter in the data movie by Eq. (10) is $M_{qe} =$ 24.361, and its value in simulation is 23.986. The average total number of activations for all emitters in the data movie by Eq. (11) is $M_{at} = 12181.094$, and its value in simulation is 11993.

In the simulation, the activation state $a_m(n)$ for each emitter in a frame is generated by the state transition diagram in Fig. 2. The number of activated emitters with $a_m(n) = 1$ in each frame

is shown in Fig. 5. The average number $M_a(n)$ of activated emitters over all M emitters by Eq. (12) is also shown. $M_a(n)$

well predicts the number of activated emitters and the photobleaching tendency with respect to frame n.

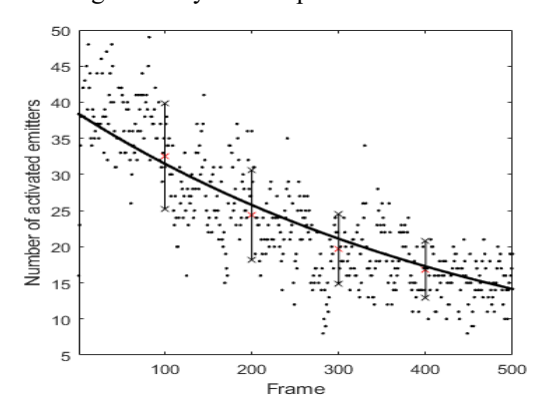


Fig. 5. Number of activated emitters vs. frame n in simulation. The sample mean is denoted by the red crosses and the mean \pm standard deviation is denoted by the black crosses. The curve is the estimated mean $M_a(n)$ by Eq. (12).

As shown in Fig. 6, once activated, emitters usually retain in the activated state for 2 to 4 consecutive frames. Since the standard deviation of PSF is $\sigma \cong 108.81$ and pixel size is equal to $D_y = 128$ nm, the Gaussian PSF effectively takes about 5×5 pixels. The data frames suffer from pixelization and noise.

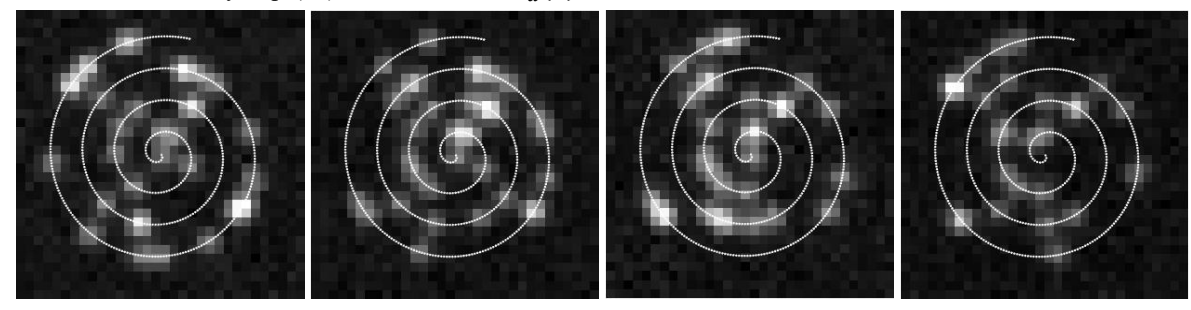


Fig. 6. From left to right are frames 104, 105, 106, and 107 with the number of activated emitters equal to 34, 35, 30, and 27. The emitter locations on the helix are shown by the white dots. Emitter 1 is located at the inner end of the helix, emitter 500 is located at the outer end of the helix, and the other emitters are placed in order on the helix. Emitter 2 is activated in frames 104, 105, and 106. Emitter 20 is activated in all four frames.

B. Cycled Illumination

In the simulation of the cycled illumination with 3D imaging, the 3D Gaussian PSF with astigmatism is applied. The following parameter values are used. (a) Data frame: For the 3D Gaussian PSF, c = 205, d = 290, $\sigma_{x0} = 140$ nm, $A_x = 0.05$, $B_x = 0.03$, $\sigma_{y0} = 135$ nm, $A_y = -0.01$, $B_y = 0.02$. The size of the field of view is $L_x = L_y = 4096$ nm, pixel size is $D_x = D_y =$ 128 nm, frame size is $K_x = K_y = 32$ pixels, and axial depth is $L_z = 400$ nm. Frame time is $D_t = 0.01$ sec, emitter intensity is I = 240000 photons/sec, and the average photon count per frame per emitter is $D_t I = 2400$ photons. The mean of Poisson noise is b = 0.3, and then $\gamma_p = 60000$. The Gaussian noise has mean $\mu = 5$ and variance G = 3 photons/sec/nm², and then $\gamma_q = 100000$. The ratio of emitter intensity and total noise is $\gamma = 37500$. For $z_0 = 0$, $\sigma_x(z_0) = 172.88$ nm, $\sigma_y(z_0) =$ 165.79 nm, and then the total SNR is SNR = $10\log_{10}[\gamma/(\sigma_x(z_0)\sigma_y(z_0))] - 11.02 \cong 1.219 \text{ (dB)}$ which is in the range of middle SNRs in practice. (b) *Emitters*: M = 500 emitters are located on a 3D helix as shown in Fig. 7. The distance between adjacent emitters is 40 nm.

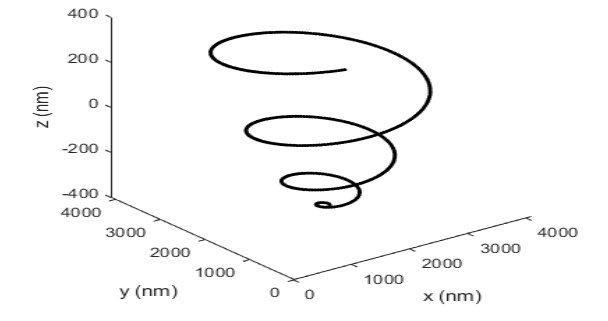


Fig. 7. 500 emitters are located on a 3D helix.

(c) Emitter activation process: The data movie has N = 500 frames, and then the acquisition time is $D_t N = 5$ sec including both the A-frames and D-frames. The mean time of photoactivatable emitter is $t_2 = 5$ sec, and then $p_2 = 0.998$. For A-frames, the mean time of emitter deactivation is $t_{A0} = 0.015$ sec, and then $p_{A0} = 0.513$. The mean time of emitter activation is $t_{A1} = 0.02$ sec, and then $t_{A1} = 0.607$. Then the

state transition probabilities are $a_{0,0} = 0.512$, $a_{1,0} = 0.486$, $a_{0,1} = 0.393$, $a_{1,1} = 0.605$, $a_{2,0} = 0.002$, and $a_{2,1} = 0.002$.

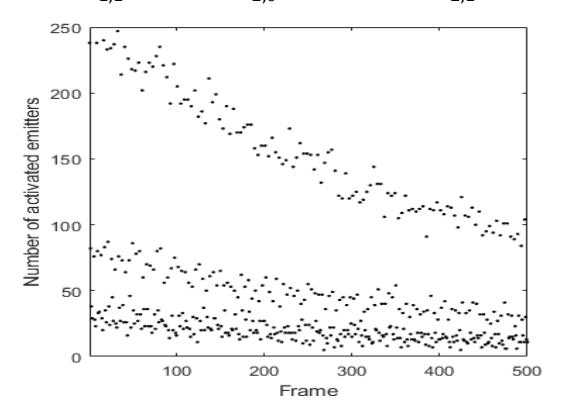


Fig. 8. Number of activated emitters in each frame.

For D-frames, the mean time of emitter deactivation is $t_{D0} = 0.30$ sec, and then $p_{D0} = 0.967$. The mean time of emitter activation is $t_{D1} = 0.008$ sec, and then $p_{D1} = 0.287$. Then the state transition probabilities are $d_{0.0} = 0.965$, $d_{1.0} = 0.0327$,

 $d_{0,1} = 0.712$, $d_{1,1} = 0.286$, $d_{2,0} = 0.002$, and $d_{2,1} = 0.002$. The average number of photoactivatable frames per emitter in simulation is $N_2 = 316.742$. The average number of activations per emitter in simulation is $M_{ae} = 60.792$. The average total number of activations for all emitters in simulation is $M_{at} = 30396$.

As shown in Fig. 7, M = 500 emitters are located on a 3D helix. In the simulation, emitters are illuminated in cycles. Each cycle consists of one A-frame followed by three D-frames. The emitters are activated according to the state transition diagram in Fig. 4. The number of activated emitters in all N = 500 frames are shown in Fig. 8. It is apparent that in the A-frames the number of activated emitters is much larger than that in the D-frames. In each cycle, the number of activated emitters decreases in order of the three D-frames.

Fig. 9 shows four frames in cycle 27. The first frame, i.e., frame 105, is an A-frame and has a much larger number of activated emitters than in the following D-frames. In the three D-frames, i.e., frames 106, 107, and 108, the number of activated emitters decreases in order.

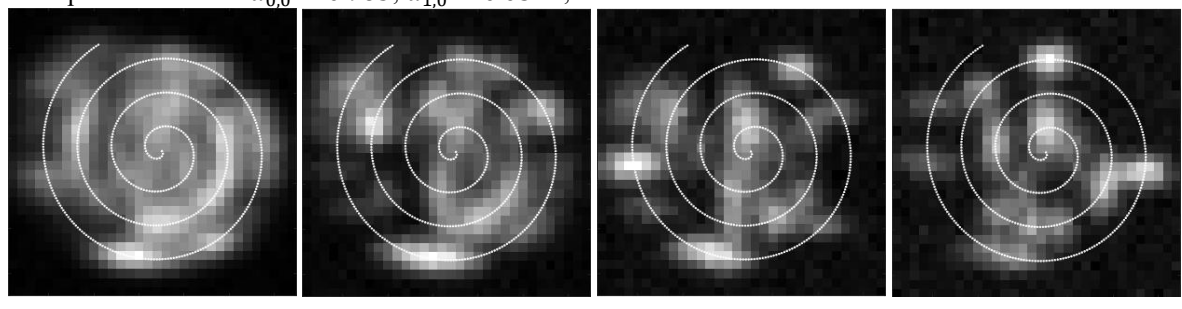


Fig. 9. From left to right are frames 105, 106, 107, and 108 with the numbers of activated emitters equal 192, 65, 33, and 21. Emitter 1 is located at the inner end of the helix, emitter 500 is located at the outer end of the helix, and the other emitters are placed in order on the helix. Emitters 20, 21, and 25 are activated in all four frames.

Note that $\sigma_x(z) < \sigma_y(z)$ for $z \ll -1$, and $\sigma_x(z) > \sigma_y(z)$ for $z \gg 1$. The emitters with a small number m have $z_m \ll -1$, and then $\sigma_x(z_m) < \sigma_y(z_m)$. On the other hand, the emitters with a large number m close to M = 500 have $z_m \gg 1$, and then $\sigma_x(z_m) > \sigma_y(z_m)$. The property is demonstrated in Fig. 9.

IV. CONCLUSIONS

It is important to establish well-reasoned models of data movies in superresolution microscopy (SRM) in order to develop advanced localization algorithms to achieve a high quality of SRM images. For the continuous illumination, the state transition probabilities are derived by the first order of kinetics of emitter activations. The stationary state probabilities in the photoactivatable time and the average number of activated emitters in a frame are derived. For the cycled illumination, a novel model of state transition is proposed, which is composed of the activation frames and followed deactivation frames in each cycle. An emitter is more likely to be activated in an activation frame than in a deactivation frame. The state transition probabilities for both types of frames are derived. Simulations of both types of illuminations with 2D and 3D imaging are carried out with incorporation of our previously proposed model of frames. The results demonstrate that both models for both types of illuminations well capture the photodynamic of photoactivatable molecules in practice. The derived formula for the average number of activated emitters predicts that in simulation. The models and the custom MATLAB codes can be broadly applied in simulations of SRM systems.

ACKNOWLEDGEMENT

The views and conclusions contained in this document are those of the author and should not be interpreted as representing the official policies, either expressed or implied, of the Army Research Office or the U.S. Government. The U.S. Government is authorized to reproduce and distribute reprints for Government purposes notwithstanding any copyright notation.

REFERENCES

- E. Betzig, G. H. Patterson, R. Sougrat, O. W. Lindwasser, S. Olenych, J. S. Bonifacino, M. W. Davidson, J. Lippincott-Schwartz and H. F. Hess, "Imaging intracellular fluorescent proteins at nanometer resolution," *Science*, vol. 313, no. 5793, p. 1642–1645, 15 Sept. 2006.
- [2] M. J. Rust, M. Bates and X. Zhuang, "Sub-diffraction-limit imaging by stochastic optical reconstruction microscopy (STORM)," *Nat. Methods*, vol. 3, no. 10, pp. 793-796, Oct. 2006.

- [3] S. T. Hess, T. P. Girirajan and M. D. Mason, "Ultra-high resolution imaging by fluorescence photoactivation localization microscopy," *Biophys. J.*, vol. 91, no. 11, p. 4258–4272, 1 Dec. 2006.
- [4] M. Heilemann, S. v. Linde, M. Schüttpelz, R. Kasper, B. Seefeldt, A. Mukherjee, P. Tinnefeld and M. Sauer, "Subdiffraction-resolution fluorescence imaging with conventional fluorescent probes," *Angew. Chem. Int. Ed.*, vol. 47, no. 33, p. 6172–6176, 2008.
- [5] D. Sage, H. Kirshner, T. Pengo, N. Stuurman, J. Min, S. Manley and M. Unser, "Quantitative evaluation of software packages for single-molecule localization microscopy," *Nat. Methods*, vol. 12, no. 8, pp. 717-724, Aug. 2015.
- [6] D. Sage, T.-A. Pham, H. Babcock, T. Lukes, T. Pengo, J. Chao, R. Velmurugan, A. Herbert, A. Agrawal, S. Colabrese, A. Wheeler, A. Archetti, B. Rieger, R. Ober, G. M. Hagen, J.-B. Sibarita, J. Ries, R. Henriques, M. Unser and S. Holden, "Super-resolution fight club: assessment of 2D and 3D single-molecule localization microscopy software," *Nat. Methods*, vol. 16, no. 5, p. 387–395, May 2019.
- [7] Y. Sun, "Root mean square minimum distance as a quality metric for stochastic optical localization nanoscopy images," *Sci. Reports*, vol. 8, no. 1, p. 17211, Nov. 2018.
- [8] Y. Sun, "Localization precision of stochastic optical localization nanoscopy using single frames," *J. Biomed. Optics*, vol. 18, no. 11, pp. 111418-14, Oct. 2013.
- [9] Y. Sun and Y. Guan, "Effect of unknown emitter intensities on localization accuracy in stochastic optical localization nanoscopy using single frames," *JOSA A*, vol. 38, no. 12, pp. 1830-1840, 2021.

- [10] E. A. Mukamel, H. Babcock and X. Zhuang, "Statistical deconvolution for superresolution fluorescence microscopy," *Biophys. J.*, vol. 102, no. 10, pp. 2391-2400, 16 May 2012.
- [11] S. Cox, E. Rosten, J. Monypenny, T. Jovanovic-Talisman, D. T. Burnette, J. Lippincott-Schwartz, G. E. Jones and R. Heintzmann, "Bayesian localization microscopy reveals nanoscale podosome dynamics," *Nat. Methods*, vol. 9, no. 2, pp. 195-200, Feb. 2012.
- [12] L. Patel, N. Gustafsson, Y. Lin, R. Ober, R. Henriques and E. Cohen, "A hidden Markov model approach to characterizing the photo-switching behavior of fluorophores," *Ann. Appl. stat.*, vol. 13, no. 3, p. 1397, 2019.
- [13] R. M. Dickson, A. B. Cubitt, R. Y. Tsien and W. E. Moerner, "On/off blinking and switching behaviour of single molecules of green fluorescent protein," *Nature*, vol. 388, no. 6640, pp. 355-358, 1997.
- [14] M. Bates, T. R. Blosser and X. Zhuang, "Short-range spectroscopic ruler based on a single-molecule optical switch," *Phys. Rev. Lett.*, vol. 94, no. 10, p. 108101, 2005.
- [15] Y. Sun, "Information sufficient segmentation and signal-to-noise ratio in stochastic optical localization nanoscopy," *Optics Letters*, vol. 45, no. 21, pp. 6102-6105, 2020.
- [16] M. Sun and Y. Sun, "Information sufficient segmentation and signal-tonoise ratio for 3D astigmatism stochastic optical localization nanoscopy," *Electronics Letters*, vol. 58, no. 2, pp. 58-60, 2021.